

The amide oxygen donor. Metal ion coordinating properties of the ligand nitrilotriacetamide. A thermodynamic and crystallographic study

Laura A. Clapp,^a Chynthia J. Siddons,^a Donald G. VanDerveer,^b Joseph H. Reibenspies,^c S. Bart Jones^a and Robert D. Hancock^{*a}

Received 25th August 2005, Accepted 12th January 2006

First published as an Advance Article on the web 25th January 2006

DOI: 10.1039/b512017a

The metal ion coordinating properties of ntam (nitrilotriacetamide) are reported. The protonation constant (p*K*) for ntam is 2.6 in 0.1 M NaClO₄ at 25 °C. Formation constants (log *K*₁) in 0.1 M NaClO₄ at 25 °C, determined by ¹H NMR and UV-Vis spectroscopy are: Ca(II), 1.28; Mg(II), 0.4; La(III), 2.30; Pb(II), 3.69; Cd(II), 3.78; Ni(II), 2.38; Cu(II), 3.16. The measured log *K*₁ values for the ntam complexes are discussed in terms of the low basicity of the N-donor, as evidenced by the p*K*, and the effect of metal ion size on complex stability. The amide O-donors of ntam lead to the stabilization of complexes of large metal ions (Pb(II), Cd(II), La(III), Ca(II)) relative to log *K*₁ for the NH₃ complexes, while for small metal ions (Ni(II), Cu(II)) the amide O-donors lead to destabilization. This is discussed in terms of the role of chelate ring size in controlling metal ion size-based selectivity. The structures of [Pb(ntam)(NO₃)₂]₂ (**1**) and [Ca₂(ntam)₃(H₂O)₂](ClO₄)₄·3H₂O (**2**) are reported. For **1**: triclinic, space group *P* $\bar{1}$, *a* = 7.4411(16), *b* = 9.0455(19), *c* = 11.625(3) Å, α = 69.976(4), β = 79.591(4), γ = 67.045(3)°, *Z* = 2, *R* = 0.0275. For **2**: monoclinic, space group *P*2₁/*c*, *a* = 10.485(2), *b* = 11.414(2), *c* = 38.059(8) Å, β = 92.05(3)°, *Z* = 4, *R* = 0.0634. Structure **1** is dimeric with two Pb atoms linked by bridging O-donors from the two ntam ligands. The coordination sphere consists of one N-donor and 3 O-donors from the ntam ligand, two O-donors from nitrates, and one bridging O-donor. The variation in bond length suggests a stereochemically active lone pair of electrons on the Pb. Structure **2** consists of two Ca(II) ions held together by 3 bridging O-donors from ntam groups. One Ca is 9-coordinate with two ntam ligands present, plus one bridging O-donor from the other Ca(II) ntam complex. The other Ca is 8-coordinate, with a single coordinated ntam, plus two coordinated H₂O molecules, and two bridging O-donors from the other half of the complex. The role of M–O=C bond angles in controlling selectivity for metal ions on the basis of their size is discussed.

Introduction

The oxygen donor atoms of amide groups are of great importance in biology, where they bind Ca²⁺ in Ca-selective proteins,¹ and are the donor atoms in potassium ion channels,² and probably also³ Ca²⁺ and Na⁺ ion channels. At the same time, amide donor ligands are of considerable importance in the extraction and separation of lanthanide and actinide ions.⁴ Despite this, very little has been reported⁵ that would allow for characterization of the metal ion binding properties of amide donor ligands. Structural studies have been reported for complexes^{6,7} of the tripodal amide donor ligand ntam (see Fig. 1 for abbreviations of ligands) and its N-substituted derivatives.^{8–14} The latter have amide groups coordinated to metal ions through the deprotonated N-donors of the amides. The tripodal nature of ntam-type ligands appears to be able to force less common coordination numbers (C.N.) on metal ions, particularly trigonal-bipyramidal 5-coordination as

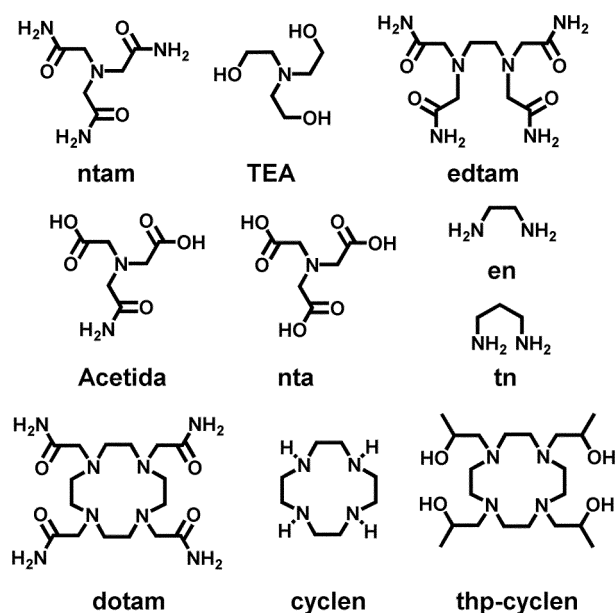


Fig. 1 Ligands discussed in this paper.

^aDepartment of Chemistry and Biochemistry, University of North Carolina at Wilmington, Wilmington, North Carolina, 28403, USA. E-mail: hancockr@uncw.edu

^bDepartment of Chemistry, Clemson University, Clemson, South Carolina, 29634, USA

^cDepartment of Chemistry, Texas A & M University, College Station, Texas, 77843, USA

found for Ni(II),¹³ Mn(III),¹⁰ and Fe(III).⁸ A recent study¹⁵ of the ligand edtam, which has four amide donors, has shown that there is a considerable increase in the formation constant, $\log K_1$, as compared to the en complexes, which is largely size-related. Thus, large metal ions (metal ions with ionic radii¹⁶ $r^+ \geq 1.0 \text{ \AA}$) such as Ca^{2+} or La^{3+} show large increases in $\log K_1$ for the edtam complexes as compared to the en complexes, whereas small metal ions such as Mg^{2+} or Ni^{2+} ($r^+ \leq 1.0 \text{ \AA}$) show only modest increases in $\log K_1$, or even decreases (Cu^{2+}). The metal ion coordinating properties of amide groups are not only of interest because of their importance in biology,¹⁻³ but are also of interest in relation to the metal ion coordinating properties of other neutral oxygen donors¹⁷⁻²⁴ such as alcoholic or ether oxygen donors. Addition of donor groups containing neutral oxygen donors causes in general¹⁷⁻²⁴ an increase in $\log K_1$ for large metal ions, and a decrease in $\log K_1$ for small metal ions. This is not simply a factor of exceeding the coordination number of small metal ions, but occurs even where a single neutral oxygen donor is added, and the accompanying increase in C.N. is only from 2 to 3. Crown ethers only complex well with large metal ions, and this is simply the extreme case of the rule that neutral oxygen donors favour complexation with large metal ions, since crown ethers have only neutral oxygen donors.²⁵ The ligand dotam, which is a tetraazamacrocycle with pendant acetamide groups, shows the same pattern in $\log K_1$ as does edtam, in that large metal ions show²⁶ large increases in $\log K_1$ relative to the parent amine cyclen, while small metal ions do not.

In this paper are reported the protonation constant of ntam, and its formation constants with the large metal ions Ca^{2+} , Pb^{2+} , and La^{3+} , the small metal ions Mg^{2+} , Cu^{2+} , and Ni^{2+} , and the intermediate sized metal ion Cd^{2+} . Also reported is a structural study of the Ca(II) and Pb(II) complexes of ntam, aimed at understanding the factors controlling metal ion selectivity in these complexes.

Experimental

Materials

The ligand ntam was synthesized by a literature method.²⁷ Metal perchlorates and nitrates were obtained from Aldrich in at least 99% purity, and used as received.

Synthesis of $[\text{Pb}(\text{ntam})(\text{NO}_3)_2] \cdot 2$ (1)

A 1 : 1 stoichiometric mixture of ntam and $\text{Pb}(\text{NO}_3)_2$ in MeOH was allowed to stand in a beaker covered with Parafilm. After a few days colourless crystals of **1** were deposited. Elemental analyses: Calc. for $\text{C}_6\text{H}_{12}\text{N}_6\text{O}_9\text{Pb}$: C, 13.85; H, 2.33; N, 16.16%. Found: C, 14.02; H, 2.27; N, 16.32%.

Synthesis of $[\text{Ca}_2(\text{ntam})_3(\text{H}_2\text{O})_2](\text{ClO}_4)_4 \cdot 3\text{H}_2\text{O}$ (2)

A solution of ntam (0.94 g) in a minimum amount of hot water was added dropwise to a solution of $\text{Ca}(\text{ClO}_4)_2 \cdot 4\text{H}_2\text{O}$ (1.56 g) in cold water, and was allowed to stand in a beaker covered with Parafilm. After a few days colourless crystals of **2** were deposited. Elemental analyses: Calc. for $\text{C}_{18}\text{H}_{46}\text{N}_{12}\text{O}_{30}\text{Cl}_4\text{Ca}_2$: C, 19.09; H, 4.09; N, 14.84%. Found: C, 18.92; H, 4.23; N, 14.86%.

Formation constant determination

The protonation constant ($\text{p}K$) of ntam was determined by glass electrode potentiometry by standard methods.²⁸ This was rather low at $\text{p}K = 2.6$, which rendered glass electrode potentiometry unsuitable for measuring formation constants of the metal ions, particularly those where $\log K_1 > 2.6$. The $\log K_1$ values for the Mg^{2+} , Ca^{2+} , Cd^{2+} , and La^{3+} complexes was determined from the shift of the 3.44 ppm band of the ^1H NMR spectrum of ntam in a 10 : 90 D_2O - H_2O mixture as a function of M^{n+} concentration, in 0.1 M NaClO_4 to control the ionic strength. It is not necessary to conduct these experiments in pure D_2O , since the 3.44 ppm band of ntam is well away from the HOD band (~ 5 ppm). 10% D_2O is needed to shim the instrument. The shifts on complex formation were quite small—from 3.44 ppm in the free ligand, to as much as 3.54 ppm in the complex (La^{3+}). The experiment consisted of recording the ^1H NMR spectrum of the free ligand, and then as a function of increasing metal ion concentration. Analysis of the data was quite straightforward, and was carried out in EXCEL.²⁹ Values of \bar{n} (L), the average number of metal ions bound to the ligand are calculated from

$$\bar{n}(\text{L}) = (\delta(\text{obs}) - \delta^\circ) / (\delta^\infty - \delta^\circ) \quad (1)$$

where $\delta(\text{obs})$ is the shift observed for each different metal ion concentration, δ° is the shift for the free ligand, and δ^∞ is the shift for the fully formed complex. A theoretical curve of $\bar{n}(\text{L})$ versus $[\text{M}]$ (the free metal ion concentration) was then calculated from

$$\bar{n}(\text{L}) = K_1[\text{M}] / (K_1[\text{M}] + 1) \quad (2)$$

where K_1 is the formation constant for formation of the complex. The values of K_1 and δ^∞ were then iterated to minimize the standard difference between calculated and experimental values of $\bar{n}(\text{L})$. In Fig. 2 is shown the curve for the equilibrium between Ca^{2+} and ntam, calculated from $\log K_1 = 1.28$, and the experimental points. The last point at $[\text{Ca}^{2+}] = 1.0 \text{ M}$ is virtually the same as the iterated value of δ^∞ . The $\log K_1$ value reported is based only on the points obtained at lower $[\text{Ca}^{2+}]$, so that an ionic strength of 0.1 could be maintained, although it is interesting that points at higher $[\text{Ca}^{2+}]$, and hence higher ionic strength, also fit the curve quite well. The good fit for all the points, except the last one, possibly reflects the lower sensitivity of $\log K_1$ for a neutral ligand such as ntam to change in ionic strength. Similar results were also obtained for Cd^{2+} , Mg^{2+} and La^{3+} .

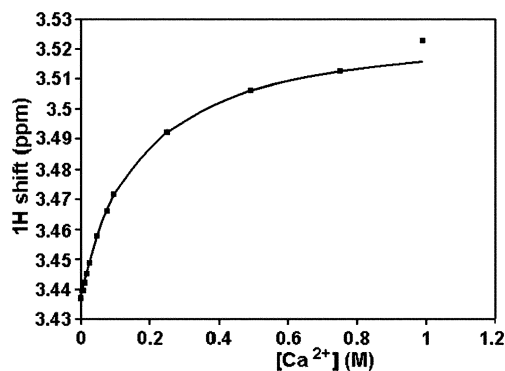


Fig. 2 Variation of the ^1H NMR shift for the $-\text{CH}_2-$ protons of ntam as a function of Ca^{2+} concentration. The solid line is a theoretical curve fitted as described in the text for a $\log K_1$ of 1.28.

UV-Vis log *K* determinations

Both Cu(II) and Ni(II) have d–d transitions in the visible part of the electronic spectrum, and these can be routinely used for stability constant determinations.²⁸ Solutions of 10^{−3} M Cu²⁺ gave bands in the 600 nm region of the spectrum that changed strongly upon addition of excess ntm, and it was found that the variation of the absorbance of these bands with ntm concentration could be simply analyzed to give log *K*₁, much as was done for the NMR shifts above, but using absorbances at three different wavelengths to calculate log *K*₁. Similar results were obtained for Ni(II), except that 10^{−2} M Ni²⁺ was used to obtain sufficiently intense bands. The spectrum of a 1 : 1 solution of Cu(II)–ntm was also recorded from pH 4–10 to obtain hydrolysis constants (p*K*_a) for the complex.

Pb(II) is usually thought of as being ‘UV-silent’, since it has a filled d¹⁰ shell. However, intense bands occur³⁰ in the 200–300 nm range of the electronic spectrum due to charge transfer transitions involving the ‘lone pair’ on the Pb(II). The variation of these bands as a function of added ntm concentration is seen in Fig. 3. Large changes in absorbance occurred, which were analyzed as two successive complex formation reactions using EXCEL.²⁹ The formation constants determined here are listed in Table 1.

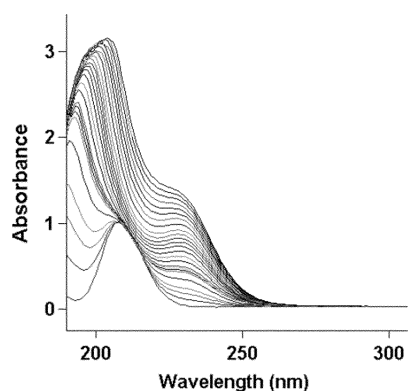


Fig. 3 Variation of the charge transfer band of Pb(II) (10^{−4} M) as a function of added ntm ligand. The lowest intensity spectrum with a band at about 210 nm is for the free Pb²⁺ ion. The highest intensity band occurs for 0.0015 M added ntm. The set of spectra represents two successive equilibria. The lower intensity set, where the band at 210 nm changes very little on its longer wavelength side, corresponds to the formation of the mono complex, while the subsequent set of spectra at higher intensity corresponds to the formation of the bis-ntm complex. Spectra recorded in 0.1 M NaClO₄ to provide a constant ionic strength.

Molecular structure determination

Bruker SMART 1 K (structure **1**) and Rigaku Mercury (structure **2**) diffractometers, using the omega scan mode, were employed for crystal screening, unit cell determination, and data collection. The structures were solved by direct methods, and refined to convergence.³¹ No absorption corrections were made. Some details of the structure determinations are given in Table 2, and crystal coordinates and details of the structure determinations of **1** and **2** have been deposited with the CSD (Cambridge Structural Database).³² CCDC reference numbers 282118 and 282119. For crystallographic data in CIF or other electronic format see DOI: 10.1039/b512017a A selection of bond lengths and angles for **1** and **2** are given in Tables 3 and 4.

Table 1 Protonation and formation constants of the ligand ntm at 25.0 °C and ionic strength 0.1 M NaClO₄

Equilibrium	log <i>K</i> ₁	Method	Reference
H ⁺ + OH [−] ⇌ H ₂ O	13.78		5
L + H ⁺ ⇌ LH ⁺	2.6(1)	glass electrode	this work
L + Ca ²⁺ ⇌ CaL ²⁺	1.28(3)	NMR	this work
L + Mg ²⁺ ⇌ MgL ²⁺	0.4(1)	NMR	this work
L + Cd ²⁺ ⇌ CdL ²⁺	3.78(6)	NMR	this work
L + Pb ²⁺ ⇌ PbL ²⁺	3.69(5)	UV-Vis	this work
L + PbL ²⁺ ⇌ PbL ₂ ²⁺	2.3(1)	UV-Vis	this work
L + La ³⁺ ⇌ LaL ³⁺	2.30(7)	NMR	this work
L + Cu ²⁺ ⇌ CuL ²⁺	3.16(3)	UV-Vis	this work ^a
CuLH _{−1} ⁺ + H ⁺ ⇌ CuL ²⁺	6.38(5)	UV-Vis	this work ^b
CuLH _{−2} ⁺ + H ⁺ ⇌ CuLH _{−1} ²⁺	7.82(5)	UV-Vis	this work ^b
L + Ni ²⁺ ⇌ NiL ²⁺	2.38(5)	UV-Vis	this work ^a

^a Figures in parentheses after each log *K* value are estimated uncertainties in the last significant figure. ^b These constants refer to deprotonation of amides coordinated to Cu(II) with a change from Cu–O to Cu–N bonding (see discussion in text).

Table 2 Crystal data and structure refinement for [Pb(ntm)](NO₃)₂ (**1**) and [Ca₂(ntm)₃(H₂O)₂](ClO₄)₄·3H₂O (**2**)

	1	2
Empirical formula	C ₆ H ₁₂ N ₆ O ₉ Pb	C ₁₈ H ₄₆ N ₁₂ O ₃₀ Cl ₄ Ca ₂
Formula weight	519.41	1132.59
Temperature	110(2)	173.2(2) K
Wavelength	0.71073	0.71073 Å
Crystal system	Triclinic	Monoclinic
Space group	<i>P</i> $\bar{1}$	<i>P</i> 2 ₁ / <i>c</i>
Unit cell dimensions	<i>a</i> = 7.4411(16) <i>b</i> = 9.0455(19) <i>c</i> = 11.625(3) <i>a</i> = 69.976(4) <i>β</i> = 79.591(4) <i>γ</i> = 67.045(3)	10.485(2) Å 11.414(2) Å 38.059(8) Å 90° 92.05(3)° 90°
Volume	675.9(2)	4551.5(16) Å ³
<i>Z</i>	2	4
Goodness-of-fit on <i>F</i> ²	1.031	1.064
Final <i>R</i> indices [<i>I</i> > 2σ(<i>I</i>)]	<i>R</i> 1 = 0.0275 <i>wR</i> 2 = 0.0678	0.0634 0.1368
<i>R</i> indices (all data)	<i>R</i> 1 = 0.0351 <i>wR</i> 2 = 0.1042	0.1009 0.1535

Table 3 Selected bond lengths and angles for [Pb(ntm)](NO₃)₂ (**1**)

Lengths/Å			
Pb(1)–O(2)	2.494(6)	Pb(1)–O(3)	2.621(6)
Pb(1)–O(1)	2.654(6)	Pb(1)–N(3)	2.654(7)
Pb(1)–O(1)#1	2.688(6)	Pb(1)–O(6)	2.688(7)
Pb(1)–O(9)	2.765(6)	Pb(1)–O(4)	3.071(7)
Angles/°			
O(2)–Pb(1)–O(3)	96.4(2)	O(2)–Pb(1)–O(1)	93.1(2)
O(3)–Pb(1)–O(1)	112.8(2)	O(2)–Pb(1)–N(3)	65.0(2)
O(3)–Pb(1)–N(3)	64.5(2)	O(1)–Pb(1)–N(3)	60.5(2)
O(2)–Pb(1)–O(1)#1	83.0(2)	O(3)–Pb(1)–O(1)#1	176.8(2)
O(1)–Pb(1)–O(1)#1	64.2(2)	N(3)–Pb(1)–O(1)#1	112.5(2)
O(2)–Pb(1)–O(6)	146.1(2)	O(3)–Pb(1)–O(6)	66.0(2)
O(1)–Pb(1)–O(6)	70.0(2)	N(3)–Pb(1)–O(6)	81.1(2)
O(1)#1–Pb(1)–O(6)	112.9(2)	Pb(1)–O(1)–Pb(1)#1	115.8(2)
C(1)–O(1)–Pb(1)	112.5(5)	C(1)–O(1)–Pb(1)#1	131.7(5)
C(4)–O(2)–Pb(1)	120.6(5)	C(6)–O(3)–Pb(1)	118.9(5)

Table 4 Selected bond lengths and angles for $[\text{Ca}_2(\text{ntam})_3(\text{H}_2\text{O})_2](\text{ClO}_4)_4 \cdot 3\text{H}_2\text{O}$ (**2**)

Lengths/Å					
Ca(1)–O(2)	2.408(3)	Ca(1)–O(4)	2.409(3)	Ca(1)–O(6)	2.426(3)
Ca(1)–O(1)	2.435(3)	Ca(1)–O(3)	2.464(3)	Ca(1)–O(5)	2.497(3)
Ca(1)–O(9)	2.536(3)	Ca(1)–N(6)	2.656(4)	Ca(1)–N(2)	2.665(3)
Ca(1)–Ca(2)	3.7055(14)	Ca(2)–O(10)	2.329(4)	Ca(2)–O(11)	2.377(3)
Ca(2)–O(8)	2.381(3)	Ca(2)–O(9)	2.402(3)	Ca(2)–O(7)	2.430(3)
Ca(2)–O(3)	2.477(3)	Ca(2)–O(6)	2.498(3)	Ca(2)–N(10)	2.658(4)
Angles/°					
O(2)–Ca(1)–O(4)	82.45(10)	O(2)–Ca(1)–O(6)	139.37(11)		
O(6)–Ca(1)–O(3)	71.23(10)	O(1)–Ca(1)–O(3)	97.81(11)		
O(6)–Ca(1)–O(5)	71.77(10)	O(1)–Ca(1)–O(5)	139.68(10)		
O(9)–Ca(1)–N(6)	117.69(10)	O(2)–Ca(1)–N(2)	66.36(10)		
N(6)–Ca(1)–N(2)	126.51(11)	O(10)–Ca(2)–O(11)	102.70(15)		
O(10)–Ca(2)–O(9)	149.90(12)	O(11)–Ca(2)–O(9)	88.53(11)		
O(9)–Ca(2)–O(7)	94.95(11)	O(10)–Ca(2)–O(3)	83.57(12)		
O(10)–Ca(2)–O(6)	87.28(13)	O(11)–Ca(2)–O(6)	72.95(11)		
O(10)–Ca(2)–N(10)	144.82(13)	O(11)–Ca(2)–N(10)	80.07(12)		
O(8)–Ca(2)–N(10)	67.06(11)	O(9)–Ca(2)–N(10)	64.14(11)		
O(7)–Ca(2)–N(10)	67.37(10)	O(3)–Ca(2)–N(10)	116.06(11)		
C(13)–O(7)–Ca(2)	120.7(2)	C(16)–O(8)–Ca(2)	123.4(3)		
C(18)–O(9)–Ca(2)	123.2(3)	C(6)–O(3)–Ca(2)	140.1(3)		
C(1)–O(1)–Ca(1)	120.4(3)	C(4)–O(2)–Ca(1)	122.9(3)		
C(6)–O(3)–Ca(1)	122.5(3)	C(6)–O(3)–Ca(2)	140.1(3)		
C(7)–O(4)–Ca(1)	123.4(3)	C(10)–O(5)–Ca(1)	120.4(3)		
C(12)–O(6)–Ca(1)	120.7(3)	C(12)–O(6)–Ca(2)	141.5(3)		
C(18)–O(9)–Ca(1)	137.9(3)	Ca(2)–O(9)–Ca(1)	97.2(1)		

Results and discussion

Formation constants

The protonation constant ($\text{p}K$) of *ntam* (Table 1) is remarkably low for a tertiary aliphatic amine. However, the effect of the strong electron-withdrawing power of the acetamide substituent can be seen from the following reported protonation constants

Ligand:	<i>nta</i>	Acet- <i>ida</i>	<i>edtam</i>	<i>ntam</i>
No of acetamide substituents on N:	0	1	2	3
$\text{p}K$ of N (ref. 5, 15, and this work)	9.46	6.67	4.65	2.6

These results show clearly the steady decrease in $\text{p}K$ of the nitrogen as more acetamide groups are added. The ligand *ntam* differs from virtually all other non-aromatic ligands with sp^3 hybridized N-donors in having an N-donor of very low basicity. This is almost certain to destabilize the complexes of metal ions with high affinities for N-donors. This appears to be borne out for some of the metal ions, as seen in Table 1. A comparison of the $\log K_1$ values⁵ for NH_3 , TEA, and *ntam* is given in Table 5. The two smallest metal ions, Ni^{2+} and Cu^{2+} , which also have the highest affinity for NH_3 , and therefore for N-donors in

general, show modest decreases in $\log K_1$ in passing from the NH_3 complexes to the TEA complexes, and hence to the *ntam* complexes. It seems possible that the decrease in $\log K_1$ for the *ntam* complex of these two ions derives both from the low basicity of *ntam*, and the fact that neutral O-donors cause¹⁹ drops in $\log K_1$ for small metal ions. The small Mg^{2+} ion has a low affinity for NH_3 , and accordingly does not show a decrease in $\log K_1$ with *ntam*. The large metal ions Ca^{2+} , La^{3+} , and Pb^{2+} , and the borderline large Cd^{2+} , all show modest increases in $\log K_1$ with the *ntam* as compared to the NH_3 and TEA complexes. This possibly reflects the lower affinity that these ions have for N-donors compared to Ni^{2+} and Cu^{2+} , but also their large size. Use of neutral oxygen donors to increase affinity for complexes of large size metal ions has been demonstrated many times.^{17–24} What is seen here is that the amide oxygen donors, as in *ntam*, are able to increase $\log K_1$ more than the alcoholic oxygen donor, as found in TEA complexes. This is in accord with the idea²⁶ that the amide oxygen donor is a stronger Lewis base than the alcoholic oxygen. A contributing factor to the observation that neutral oxygen donors stabilize complexes with larger metal ions lies in the geometry of chelate rings.²⁵ The minimum strain geometry³³ for 5-membered and 6-membered chelate rings is shown in Fig. 4.

Table 5 Comparison of formation constants of NH_3 , TEA (triethanolamine) and *ntam*. Also given are the ionic radii of the metal ions

Lewis acid	H^+	Pb^{2+}	La^{3+}	Ca^{2+}	Cd^{2+}	Mg^{2+}	Ni^{2+}	Cu^{2+}
Ionic radius (r^+) ^a /Å	—	1.19	1.03	1.00	0.95	0.74	0.67	0.57
$\log K_1$ (NH_3) ^b	9.26	1.6	(0.4)	0.1	2.65	0.24	2.83	4.08
$\log K_1$ (TEA) ^b	7.85	3.39	—	0.78	2.70	0.24	2.76	4.07
$\log K_1$ (<i>ntam</i>)	2.6	3.69	2.30	1.28	3.78	0.4	2.38	3.16
$\log K_1$ (<i>ntam</i> – NH_3) ^c	–6.7	2.1	1.9	1.2	1.1	0.2	–0.4	–0.8

^a Ref. 16. The ionic radii refer to coordination number 6, except for $\text{Cu}(\text{II})$, which is for coordination number 4. ^b Reference 5. ^c This corresponds to the equilibrium $\text{M}(\text{NH}_3)^{n+} + \text{ntam} \leftrightarrow \text{M}(\text{ntam})^{n+} + \text{NH}_3$.

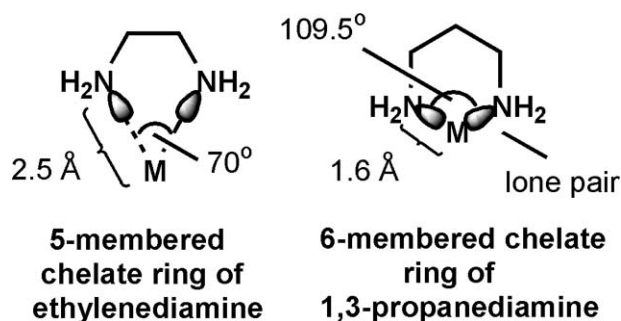


Fig. 4 Minimum strain geometries for 5- and 6-membered chelate rings.

In essence, ligands that form 5-membered chelate rings are better preorganized for coordinating with large metal ions, while those that form 6-membered chelate rings are better preorganized for coordinating with small metal ions. It is important to understand that this does not just apply to chelate rings such as the above en and tn chelate rings. It applies to any chelate rings, even planar chelate rings with delocalized electronic systems, such as the 6-membered acetylacetonate compared to the 5-membered tropolonate chelate ring. The design principle also extends to 4-membered chelate rings, which are preorganized to complex best with the largest metal ions. The presence of 4-membered chelate rings formed between Ca^{2+} and chelating carboxylates from glutamate or aspartate residues in the binding sites of Ca-selective proteins would seem to be an important factor^{15,34} in producing selectivity for the large Ca^{2+} ion over the small Mg^{2+} ion. In the case of ntam, the ligand forms three 5-membered chelate rings on complex formation, and this at least in part should account for the greater stabilization of the ntam complexes compared to the NH_3 complexes observed in Table 5 for larger metal ions.

A referee has queried the non-observation of a bis-ntam complex for Ca(II) in solution, when one is reported for Pb(II). This is particularly so when the structure reported here for the Pb(II)–ntam complex is for a mono-ntam complex, although it is acknowledged that there is no necessary correspondence between solution and solid state species. There is in fact a reported structure⁷ for a bis-ntam complex of Pb(II), supporting the observation of such a complex in solution by UV-Vis spectroscopy here. The $\log K_1$ value for Ca(II) with ntam at 1.28 is rather small, so that the non-observation of a bis-ntam complex here would reflect the fact that $\log K_2$ would be expected to be much smaller than 1.28, and the concentration of ntam was never high enough to cause the formation of such a weak complex. Fig. 3 shows the use of the charge-transfer bands of Pb(II) to determine its formation constants with ntam. As far as we are aware this is the first such use of these bands, and this study shows how useful an approach this is. The bands are intense, making study of complexes at low concentration practicable, which is advantageous in studying complexes with ligands of low solubility. The bands are also very sensitive to complex formation. One sees the very large increase in absorbance produced in Fig. 3 by the formation of the ntam complexes. One should note that as the ntam is added, the first nine spectra as absorbance increases are the region where the mono-ntam complex of Pb(II) is forming, and thereafter the bis-ntam complex is being formed. The concentration intervals in Fig. 3 as the complexes form are approximately 0.000 05 M in ntam, ranging from no ntam added to a total of 0.0015 M ntam

in the most intense spectrum. The $\log K$ values for Pb(II) with ntam were not studied by ^1H NMR as UV-Vis spectroscopy appeared to be preferable. For optimal determination of $\log K$ by spectroscopic means, the concentration of the ligand should not be too far from the reciprocal of the K value to be determined, so that in calculating the concentrations of the ligand bound to the metal ion, and of the free ligand, one is not using small differences between large numbers. Thus, for NMR, $\log K$ values of about 2 as found for Ca(II) and La(III) were ideal when working with 0.01 M ntam.

A further point of interest is the deprotonations that are evident in the UV-Vis spectrum of the Cu(II)–ntam complex as the pH is raised. It is possible that at least one of these might be due to deprotonation of a coordinated water. However, there are several structures^{8–11} of complexes of deprotonated ntam analogues where all three amides are deprotonated, and the metal ions are bound to the amide groups through the deprotonated nitrogens. We therefore expect that the same would occur here with the Cu(II)–ntam complex. The idea that bonding of the Cu(II) is taking place through the deprotonated nitrogens of the ntam is also supported by the intense purple colour of the resulting solution containing these complexes, concomitant with more covalent binding to the N-donors rather than the more ionically bound oxygens of hydroxide ions.

The structures of the Pb(II) and Ca(II) ntam complexes

The structures of the complex cations of **1** and **2** are shown in Fig. 5 and 6. Structure **1** is a dimeric complex with two Pb(II) ions, each coordinated to 1 N-donor and 3 O-donors of ntam, plus a bridging O-donor from the ntam of the other half of the dimer. Two NO_3^- ions are coordinated to each Pb(II), giving a coordination number of 7 for each Pb(II) if these are regarded as being unidentate. However, at least one of the nitrates may be regarded as chelating in an asymmetrical manner, with one shorter Pb–O(6) = 2.688 Å, and a longer Pb–O(4) = 3.071 Å, which would raise the C.N. to 8. The long Pb–O(4) bond is typical of bonds close^{35,36} to the stereochemically active lone pair on Pb(II), and

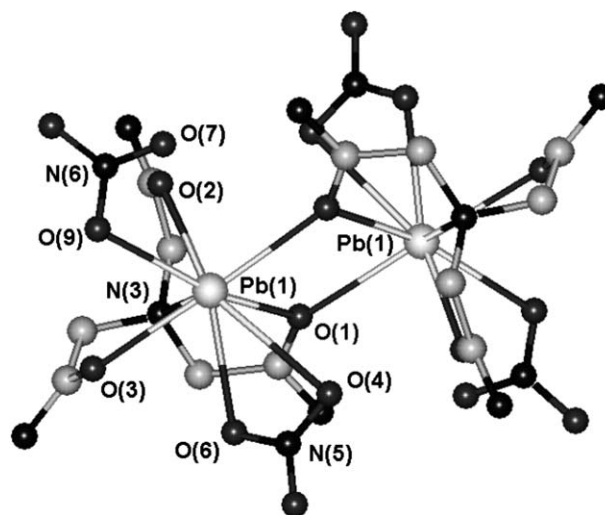


Fig. 5 The complex $[\text{Pb}_2(\text{ntam})_2(\text{NO}_3)_4]$ (**1**), showing the numbering scheme for the donor atoms coordinated to Pb(II), plus some other heteroatoms. H atoms are omitted for clarity. The Pb–Pb separation is 4.525 Å.

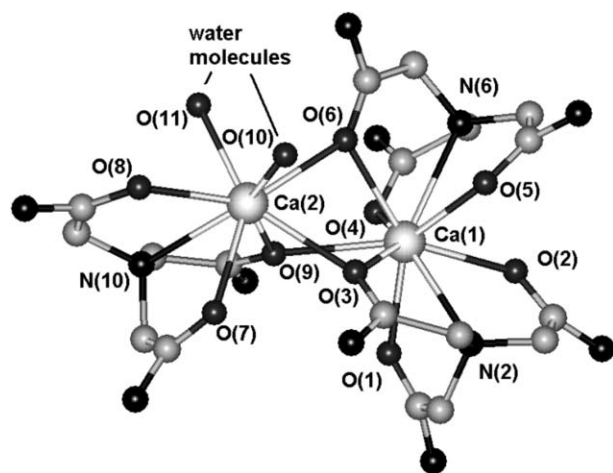


Fig. 6 The complex cation $[\text{Ca}_2(\text{ntam})_3(\text{H}_2\text{O})_2]^{4+}$ of **2**, showing the numbering scheme of the donor atoms coordinated to the two Ca ions. H atoms are omitted for clarity.

is shorter than the sum of the van der Waals radii³⁷ ($\text{Pb} = 2.00$, $\text{O} = 1.50$ Å). This is particularly true, since the $\text{Pb}(\text{II})$ ion does not appear to be spherical where the lone pair is stereochemically active, but ovoid.^{36,38} The variation of the Pb-L bond lengths is such that a stereochemically active lone pair appears to be present in **1**. The structural features associated with a stereochemically active lone pair are:³⁶

1) There may be a gap in the coordination sphere, with no donor atoms within reasonable (less than ~ 4.0 Å) bonding distance of the Pb, or the Pb-L bonds located over the proposed position of the lone pair are very long. Thus, $\text{Pb}(1)\text{-O}(4) = 3.07$ Å is rather long, and $\text{O}(4)$ is quite close to the possible site of the lone pair.

2) The Pb-L bonds which are furthest from the site of the lone pair are shorter than the other bonds in the complex, once corrected for differing ionic radii of the donor atoms.

3) The bonds become progressively shorter as one moves from the site of the lone pair to a position opposite the lone pair.

The lone pair would be approximately at right angles to the plane of the paper, so that one might be looking down on the site of the lone pair on the left-hand side of the two Pb atoms in Fig. 5. As is usually found with a stereochemically active lone pair, the bonds opposite this site are short. In this case, $\text{Pb-N}(3)$ and $\text{Pb-O}(2)$ are the shortest of the Pb-L bonds, once 0.06 Å is subtracted to correct^{36,38} for the larger ionic radius¹⁶ of N as compared to O. The short $\text{Pb-N}(3)$ and $\text{Pb-O}(2)$ bonds suggest that the lone pair may be approximately at 180° to a line bisecting the $\text{N}(3)\text{-Pb-O}(2)$ angle. The O donors close to the site of the lone pair would be rather long, and this might account for the long $\text{Pb-O}(4)$ bond, since $\text{O}(4)$ is quite close to this site. The second NO_3^- may be truly unidentate, since its second closest oxygen to Pb, $\text{O}(7)$, is at a rather long distance of 3.638 Å, and $\text{O}(7)$ is not particularly close to the site of the lone pair. There do not appear to be any donor atoms within 4.0 Å of the $\text{Pb}(\text{II})$ above the site we have proposed here for the stereochemically active lone pair, in accord with requirement (1) above which states that there may be a gap in the coordination sphere at the site of the lone pair.

The $[\text{Ca}_2(\text{ntam})_3(\text{H}_2\text{O})_2]^{4+}$ complex cation (Fig. 6) contains two $\text{Ca}(\text{II})$ ions in rather different environments, held together by three bridging O-donors derived from amide carbonyl groups. $\text{Ca}(1)$ has

two ntam groups coordinated to it, plus a bridging O-donor from the ntam coordinated to $\text{Ca}(2)$, giving a total C.N. of 9. $\text{Ca}(2)$ has one ntam coordinated to it, plus two water molecules, and two bridging O-donors from ntam groups from the $\text{Ca}(1)$ part of the complex cation, giving a C.N. of 8. The Ca-O bond lengths to non-bridging ntam O-donors fall in the range $2.381\text{--}2.435$ Å, with the bridging ntam O-donors being somewhat longer at $2.402\text{--}2.537$ Å. A point of interest in this structure is the Ca-O=C bond angles. It has been suggested¹⁵ that the Ca-binding sites in proteins may exert selectivity for Ca^{2+} over Mg^{2+} by structurally forcing very large M-O=C bond angles for the metal ion. A survey³⁹ of 40 structures in the protein database (PDB)⁴⁰ of Ca^{2+} ions bound in Ca-selective proteins reveals that the majority of Ca-O=C bond angles fall in the range $150\text{--}180^\circ$. This is in contrast to a molecular mechanics (MM) study⁴¹ which suggests that the strain-free Ca-O=C and Mg-O=C bond angles with coordinated amides are 140.5 and 135.1° . The Ca-O=C angle bending force constants are smaller than the Mg-O=C force constants,⁴¹ so Ca^{2+} may be better able to tolerate distortion of its M-O=C angles to larger values than Mg^{2+} . In the $\text{Ca}(\text{II})\text{-edtam}$ complex, the Ca-O=C bond angles for non-bridging amide oxygens fall in a narrow range of $120.4\text{--}123.4^\circ$. Larger bond angles are observed with bridging oxygens, being as large as 141.5° . In the case of ntam, the ligand enforces M-O=C bond angles that are smaller than the ideal values. The Pb-O=C bond angles fall in the range $112.5\text{--}120.6^\circ$. Again, an important part of the stabilization of ntam complexes relative to the NH_3 complexes of large metal ions such as Ca^{2+} may derive from the smaller Ca-O=C force constants, and hence greater tolerance of such distortion. An important aspect is also the fact that the smaller the metal ion is when part of 5-membered chelate rings, as produced by ntam, the smaller will be the M-O=C bond angle, and hence the greater the resulting steric strain. Thus, for example, for amide complexes with the small $\text{Cu}(\text{II})$ ion, the Cu-O=C bond angle to a coordinated amide that is part of a 5-membered chelate ring falls³² in the range $103.0\text{--}113.9^\circ$ (47 structures).

Conclusions

The study of ntam complexes reported here shows that 1) the acetamide groups of ntam are very electron-withdrawing, leading to a very low protonation constant of 2.6. The low basicity of the N-donor of ntam may account in part for the low $\log K_1$ values observed for metal ions such as $\text{Cu}(\text{II})$ and $\text{Ni}(\text{II})$, which have a high affinity for N-donor ligands such as NH_3 . 2) The ntam complexes of large metal ions ($r^+ > 1.00$ Å) have larger $\log K_1$ values than the triethanolamine complexes, supporting the idea that amide oxygens are stronger donors than alcoholic oxygens. 3) The amide O-donors of ntam lead to considerable stabilization of complexes of large metal ions compared to the NH_3 complexes, while complexes of small metal ions are destabilized. This is interpreted as partly due to the geometry of the 5-membered chelate rings formed by ntam, which favours coordination with large metal ions. 4) The ntam ligand coordinates *via* its O-donors to metal ions such as $\text{Ca}(\text{II})$ and $\text{Pb}(\text{II})$. In this it shows some similarity to metal ion binding sites in Ca-selective proteins, where the $\text{Ca}(\text{II})$ is usually coordinated to one or more amide oxygens. In the latter, Ca-O=C bond angles that are much larger than the ideal Ca-O=C bond angle are found, while in the ntam complexes

the M–O=C bond angles are smaller than the ideal angles. In both cases tolerance to distortion of the M–O=C bond angles, as evidenced by small M–O=C bond angle deformation force constants, may be an important factor in strong coordination to amide groups.

Acknowledgements

The authors thank the National Science Foundation (Grant # 0111131), and the University of North Carolina at Wilmington, for generous support for this work.

References

- 1 *Handbook of Metalloproteins*, ed. A. Messerschmidt, M. Cygler and W. Bode, Wiley, Hoboken, NJ, 2004, vol. 3, pp. 443–756.
- 2 Y. Jiang, A. Lee, J. Chen, V. Ruta, M. Cadene, B. T. Chait and R. MacKinnon, *Nature*, 2003, **423**, 33.
- 3 B. Hille, *Ion Channels of Excitable Membranes*, Sinauer Associates, Sunderland, MA, USA, 2001.
- 4 I. Katsuki, Y. Motoda, Y. Sunatsuki and N. Matsumoto, *J. Am. Chem. Soc.*, 2002, **124**, 629.
- 5 A. E. Martell and R. M. Smith, *Critical Stability Constant Database, 46*, National Institute of Science and Technology (NIST), Gaithersburg, MD, USA, 2003.
- 6 E. Skrzypczak-Jankun and D. A. Smith, *Acta Crystallogr., Sect. C: Cryst. Struct. Commun.*, 1994, **50**, 1585.
- 7 D. A. Smith, S. Suheck and A. A. Pinkerton, *J. Chem. Soc., Chem. Commun.*, 1992, 367.
- 8 M. Ray, A. P. Golombek, M. P. Hendrich, V. G. Young, Jr and A. S. Borovik, *J. Am. Chem. Soc.*, 1996, **118**, 6084.
- 9 M. Ray, B. S. Hammes, G. P. A. Yap, A. L. Rheingold and A. S. Borovik, *Inorg. Chem.*, 1998, **37**, 1527.
- 10 Z. Shinn, V. G. Young, Jr. and A. S. Borovik, *Chem. Commun. (London)*, 1967, 1997.
- 11 B. S. Hammes, D. Ramos-Maldonado, G. P. A. Yap, L. Liable-Sands, A. L. Rheingold, V. G. Young, Jr. and A. S. Borovik, *Inorg. Chem.*, 1997, **36**, 3210.
- 12 M. Ray, A. P. Golombek, M. P. Hendrich, G. P. A. Yap, L. Liable-Sands, A. L. Rheingold and A. S. Borovik, *Inorg. Chem.*, 1999, **38**, 3110.
- 13 B. S. Hammes, D. Ramos-Maldonado, G. P. A. Yap, A. L. Rheingold, V. G. Young, Jr and A. S. Borovik, *Coord. Chem. Rev.*, 1998, **174**, 241.
- 14 N. Yang, J. Zheng, W. Liu, N. Tang and K. Yu, *J. Mol. Struct.*, 2003, **657**, 177.
- 15 C. J. Siddons and R. D. Hancock, *Chem. Commun.*, 2004, 1632.
- 16 R. D. Shannon, *Acta Crystallogr., Sect. A: Cryst. Phys., Diffraction, Theor. Gen. Cryst.*, 1976, **32**, 751.
- 17 K. Damu, M. S. Shaikjee, J. P. Michael, A. S. Howard and R. D. Hancock, *Inorg. Chem.*, 1986, **25**, 3879.
- 18 R. D. Hancock, R. Bhavan, P. W. Wade, J. C. A. Boeyens and S. M. Dobson, *Inorg. Chem.*, 1989, **28**, 187.
- 19 R. D. Hancock and A. E. Martell, *Chem. Rev.*, 1989, **89**, 1875.
- 20 K. V. Damu, R. D. Hancock, P. W. Wade, J. C. A. Boeyens, D. G. Billing and S. M. Dobson, *J. Chem. Soc., Dalton Trans.*, 1991, 293.
- 21 R. D. Hancock, in *Perspectives in Inorganic Chemistry*, ed. A. P. Williams, C. Floriani and A. E. Merbach, VCH Publishers, Weinheim, 1992, pp. 129–151.
- 22 R. D. Hancock, *Pure Appl. Chem.*, 1993, **65**, 941.
- 23 R. D. Hancock, *J. Inclusion Phenom. Mol. Recognit. Chem.*, 1994, **17**, 63.
- 24 A. E. Martell and R. D. Hancock, *Coord. Chem. Rev.*, 1994, **133**, 39.
- 25 R. D. Hancock, *J. Chem. Educ.*, 1992, **69**, 615.
- 26 H. Maumela, R. D. Hancock, L. Carlton, J. M. Reibenspies and K. P. Wainwright, *J. Am. Chem. Soc.*, 1995, **117**, 6698.
- 27 L. Przyborowski, *Rocz. Chem.*, 1970, **44**, 1883.
- 28 A. E. Martell and R. J. Motekaitis, *Determination and Use of Stability Constants*, VCH Publishers, New York, 1989.
- 29 E. J. Billo, *EXCEL for Chemists*, Wiley-VCH, New York, 2001.
- 30 E. S. Claudio, H. A. Godwin and J. S. Magyar, *Prog. Inorg. Chem.*, 2003, **51**, 1.
- 31 E. J. Gabe, Y. Le Page, J.-P. Charland, F. L. Lee and P. S. White, *J. Appl. Crystallogr.*, 1989, **22**, 384.
- 32 *Cambridge Crystallographic Data Centre*, 12 Union Road, Cambridge CB2 1EZ, UK.
- 33 R. D. Hancock, *Acc. Chem. Res.*, 1990, **23**, 253.
- 34 R. D. Hancock and A. E. Martell, *Adv. Inorg. Chem.*, 1995, **42**, 89.
- 35 L. Shimon-Livny, J. P. Glusker and C. P. Bock, *Inorg. Chem.*, 1998, **37**, 1853, and references therein.
- 36 R. D. Hancock, J. H. Reibenspies and H. Maumela, *Inorg. Chem.*, 2004, **43**, 2981.
- 37 A. Bondi, *J. Phys. Chem.*, 1964, **68**, 441.
- 38 R. Luckay, I. Cukrowski, J. Mashishi, J. H. Reibenspies, A. H. Bond, R. D. Rogers and R. D. Hancock, *J. Chem. Soc., Dalton Trans.*, 1997, 901.
- 39 L. A. Clapp, C. J. Siddons, J. R. Whitehead, D. G. VanDerveer, R. D. Rogers, S. T. Griffin, S. B. Jones and R. D. Hancock, *Inorg. Chem.*, 2005, **44**, 8945.
- 40 H. M. Berman, J. Westbrook, Z. Feng, G. Gilliland, T. N. Bhat, H. Weissig, I. N. Shindyalov and P. E. Bourne, *Nucleic Acids Res.*, 2000, **28**, 235.
- 41 B. P. Hay, O. Clement, G. Sandrone and D. Dixon, *Inorg. Chem.*, 1998, **37**, 5887.